JOURNAL OF MATERIALS SCIENCE 13 (1978) 627–638

The sputtering behaviour of calcite

J. ADETUNJI*, D. J. BARBER
Physics Department, University of Essex, Colchester, Essex, UK

Optical and electron microscopy were used to study the effect of bombarding carbonate single crystals (mainly calcite) with argon ions from a cold cathode d.c. ion source operated at 5 kV. The sputtering yield, S, and the thickness Δ, of the amorphous surface layer formed as a result of ion irradiation were the two quantities which were determined. The electron microscope method for measuring these parameters employed simple tilting and diffraction operations and it should therefore be applicable to other types of crystal. The variation of S as a function of the angle of incidence of the ion beam to the crystal surface was measured, with the crystal rotated to minimize possible channelling effects. In separate experiments it was found that channelling occurred along the $\langle 1\,1\,\bar{2}\,0\rangle$ and $\langle \bar{4}\,4\,0\,1\rangle$ directions and that for these directions S was greatly reduced, while Δ was large. The temperature of the target crystal was also shown to be an important factor in determining S and Δ for calcite. This temperature effect is attributed to the indirect effect of chemical decomposition, with loss of carbon dioxide, rather than sputtering *sensu stricto.*

1. Introduction

In this paper we report the results of a study of the sputtering behaviour of calcite (calcium carbonate) single crystals. The high birefringence of these crystals, coupled with their excellent cleavage have enabled us to introduce novel methods of measuring the sputtering yield S, employing both optical and electron microscopy.

Our results, although only qualitative because of the limitations of the d.c. glow discharge ion source used, are nonetheless useful because of the lack of information about the sputtering of non-metals. There is now considerable data on the sputtering of elements and of metals, in particular. The comprehensive reviews by Carter and Colligon [1], Sigmund [2, 3] and Oechsner [4] summarize the essential results and indicate the following general points. The sputtering yield depends upon (a) the energy of the incident ions, (b) the masses of the incident and target ions, (c) the inclination of the ion trajectories to the target surface. In addition, it is recognized that the removal of target atoms by sputtering is accompanied by disruption of the normal structure of the subsurface target material (radiation damage) and by the creation of surface microtopography. Several theories endeavour to provide a means of calculating basic sputtering parameters, such as S, by treating radiation damage, topographic changes and modifications to surface binding energy as of secondary importance. The comparative merits of three of these theories have been considered by Tsong and Barber [5].

Another process which can be of considerable importance in determining S is the steering of ions, incident parallel to certain 'open' crystallographic directions, deep into the lattice of the target crystal. This phenomenon, known as channelling, has been studied by various workers and has been reviewed by Martynenko [6], Gemmell [7] and Carter and Grant [8].

Much interest now centres around the nature of the subsurface structure of ion-bombarded crystals and how its thickness varies with irradiation conditions. The surface is commonly described as being 'modified' by sputtering and this modification may manifest itself as either destruction of the

*Present address: Physics Department, Ahmadu Bello University, Zaria, Nigeria.

normal crystallinity (radiation damage) or enrichment of an atomic species, or both.

The creation of an amorphous surface layer on silicon by ion bombardment was first demonstrated by Gianola [9]. This was later confirmed by Mazey *et al.* [10], using electron microscopy. Later MacDonald [11] showed that ion bombardment produced a highly-disordered or an amorphous layer on germanium which became ordered if irradiation was carried out above a critical temperature. Wilson [12] demonstrated that amorphous layers could be created on compound semiconductors such as gallium arsenide as well as on elemental semiconductors. These results are in sharp contrast to the creation of defect clusters and dislocation loops in metals, as reported by Hermanne and Art [13].

The sputter-thinning of carbonates for mineralogical studies by Barber and Wenk [14] at Essex has shown that ion-damage in these compounds takes the form of an amorphous layer, as indeed it does in many silicate minerals [15, 16]. With compounds in general there is always the risk of differential sputtering of the constituent atoms, with a greatly enhanced probability if one species is volatile and significant heat is generated in the target. For example, Putnis [17] and others have commented upon the chemical decomposition or transformation of sulphides induced by ion bombardment. Naguib and Kelly [18] have reviewed the structural changes produced by ion bombardment for a large number of non-metallic compounds. They have shown that where preferential loss of one atomic species occurs, it can be correlated with the heat of atomization.

In the case of alloys there is more detailed information, most of which points to the modification of the surface layer to compensate for the preferential sputtering of one atomic species. Tarng and Wehner [19] first used Auger spectroscopy to show that the surface of a sputtered Cu/Ni alloy becomes enriched in nickel. Surface enrichment due to preferential sputtering effects has also been demonstrated in Pt Si and Ni Si by Poate *et al.* [20] using Rutherford backscattering. Ho *et al.* [21] in another Auger study of preferential sputtering in a homogeneous Cu/Ni alloy, have shown that the thickness of the modified surface layer is about 20 Å for bombardment with 2 keV Ar^+ ions.

We undertook the experiments reported here with a two-fold purpose: to explore the new methods of measuring the sputtering yield and to obtain some basic information about the interaction of ion beams with single crystals of certain carbonates, especially calcite. Bach [22] has carried out the only previous measurements of the sputtering of calcite; he compared the measured yield with theoretical values deduced using the theory of Brandt and Laubert [23].

2. Experimental

2.1. Sputtering apparatus

The work chamber for sputtering was a glass cylinder, mounted on top of a 10 cm oil diffusion pump with a liquid nitrogen trap and closed at the top with a plate on which were mounted the ion source, goniometer target table, etc. The ion source was of the d.c. glow discharge type, into which argon gas was bled via a fine dosing valve, controlled by a simple servo mechanism. The ion source was fitted with an additional electrode with a 0.5 mm diameter aperture on the work-chamber side of the cathode. This electrode collected a fraction of the ion current and was used with an electrometer and minicontroller to form a feedback system for maintaining a constant ion current. The gas dosing valve was driven via a 30:1 reducing gearbox from a 1 r.p.m. reversible motor linked to the minicontroller. By this means it was possible to maintain the ion current (plotted on a chart recorder) constant to within 2.5% over periods of several hours, despite gradual changes in the anode–cathode configuration of the ion source. The source was normally operated at 5 kV to give an ion current density at the target of 80 $\mu A\,cm^{-2}$; the ion current was measured with a double shielded Faraday cup. The ultimate vacuum attainable with the system was 1×10^{-6} torr, but owing to the throughput of argon gas the normal operating vacuum was about 5×10^{-4} torr.

Measurements showed that the half angle divergence of the ion source was $< 1°$, which is small enough for channelling effects to be studied [24]. Under the normal operating conditions the current density in the beam was found to be essentially uniform over a diameter of 4.8 mm at a distance of 4 cm from the source, where the target was located.

The goniometer target table, mentioned earlier, incorporated a small motor so that targets could be rotated during irradiation about an axis normal to the target surface. The surface could be set at inclinations to the ion beam between 0 and 90°. As alternatives to the goniometer, we also designed

and constructed target tables for target irradiation at normal incidence which permitted the target to be rotated in its plane while maintained at low temperature. Temperatures were measured with an iron-constantan themocouple located immediately below the target surface, silver 'dag' being used to achieve good thermal contact.

2.2. Methods of measuring sputtering yield

2.2.1. General

A standard method of determining the sputtering yield S, defined as the average number of target atoms ejected per incident ion, is to find the weight loss of the target produced by a known ion dose. Another method, due to Bach [22], measures the sputtered volume by means of interference optical microscopy. The methods we have used in our work can be considered as extensions of Bach's method, exploiting the birefringent character of the carbonates and the greater accuracy afforded by electron microscopy for low ion doses. The electron microscope method has the important added advantage that it appears to be the only method which can be used to determine the thickness of the amorphous surface layer formed during the sputtering of certain non-metallic targets. The majority of the results reported here relate to calcite, although some work on dolomite has also been carried out.

2.2.2. Polarizing microscope method

A thin section of an anisotropic crystal when placed between the crossed polarizers of an optical microscope will normally show interference colours. These colours arise from the recombination of waves emerging from the crystal which have been subjected to differing amounts of retardation and are therefore different in phase. The phase difference is equal to $T(n_2 - n_1)/\lambda$ where T is the section thickness, n_2 and n_1 are the refractive indices in the slow and fast directions and λ is the wavelength (see [25]). Knowing the values of n_1 and n_2 for a given crystal, section thicknesses can be gauged with some accuracy provided the difference between n_2 and n_1 is reasonably large. In practice, this is most conveniently achieved by means of a Michael–Levy chart which is a plot of section thickness versus retardation for minerals, showing the various orders of interference colours. For calcite and dolomite $(n_2 - n_1)$ has the values 0.172 and 0.185 respectively. The use of interference colours to estimate thickness before and after a timed irradiation is most accurate when the target is a thick wedge of low included angle.

We may reasonably assume that only the crystalline part of the irradiated material contributes to the interference colours; therefore the amorphous subsurface layer present after irradiation is not 'seen', nor included in the thickness measurement. We may thus write the amount of material sputtered per unit time as

$$R = \frac{T_1 - (T_2 + \Delta)}{t} \qquad (1)$$

where Δ is the thickness of the amorphous layer. If the irradiation time is long, so that $(T_1 - T_2) \gg \Delta$, the presence of the layer can be neglected. In practice this condition will be satisfied because the method is only sufficiently accurate when t, and hence $(T_1 - T_2)$, is large.

2.2.3. Transmission electron microscope method

At 100 kV the electron microscope will satisfactorily transmit through and image defect structures in thin samples (typically up to 300 nm in thickness). Use of this instrument in determining the amount of material removed by sputtering is therefore clearly dependent upon (a) making measurements of specimen thickness before and after ion irradiation at the same point and, consequently, (b) on the removal of less than 300 nm during sputtering.

In principle the measurement of specimen thickness by electron transmission can be achieved in several ways. These include stereomicrography of features which allow one to discern the top and bottom surfaces of a specimen, the use of thickness extinction fringes in thin crystals set close to a Bragg condition, and the determination of the width of the projected image of a defect which passes through the specimen at some known orientation (see [26]). We used a development of the last method, thus enabling the thickness of the amorphous layer produced by sputtering to be measured.

The manner in which the creation of the amorphous layer can be deduced is illustrated in Fig. 1. The electron micrograph in Fig. 1a, taken at 1 MeV, shows a region which is close to penetration in a crystal section of dolomite which has been made thin by the ion bombardment of both of its faces. As the selected area diffraction pattern in Fig. 1b shows, the crystal was oriented very

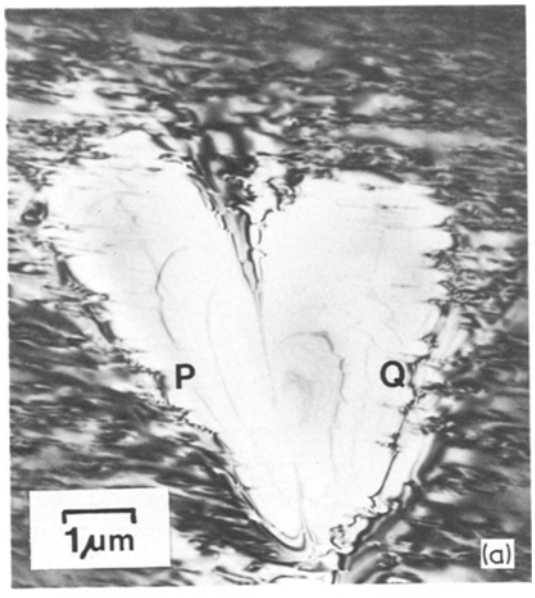

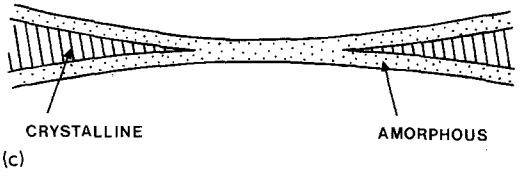

(c)

Figure 1 (a) Transmission electron micrograph (1 MeV) of ion-bombarded dolomite crystal, showing the amorphous material in an ultra-thin region, (b) selected area diffraction pattern of whole field of Fig. 1a showing remaining crystal orientation and haloes of diffuse-scattered electrons around diffraction spots (0 1 $\bar{1}$ 2 systematic row is bright), (c) sketch of section of the specimen through the line *PQ* of Fig. 1a, showing amorphous material.

close to a Bragg diffraction condition so that the 0 1 $\bar{1}$ 2 systematic diffraction row is operating. The diagram in Fig. 1c, which represents a section through the crystal, illustrates the geometry of the situation. The central region of the micrograph Fig. 1a shows very little structure; this could be partly because of kinematical effects, but in fact it is principally because its crystallinity has been largely destroyed by ion irradiation. This leads to an additional halo of diffusely scattered electrons around the diffraction spots and the undeviated main beam. Surrounding the thin central volume there is strong elastic scattering because the crystal is set at the Bragg condition and the image is consequently dark.

A planar defect, such as a twin boundary, in a crystal section or a cleavage flake, would normally extend from one surface to the other, as shown in Fig. 2a. It can be imaged in the electron microscope and, if the crystallography of the sample is established so that α is known, it can be used to determine the section thickness. However, if there is an amorphous layer below one face of the crystal section, the defect will cease to exist at the boundary between the amorphous and crystalline material, as shown in Fig. 2b. Provided some additional method can be used to establish the position of the exterior surface of the amorphous layer, it is clearly feasible to determine the layer thickness Δ, and to deduce the sputtering yield. In our experiments this requirement was met by attaching tiny polystyrene spheres of known diameter to the specimen surfaces after sputtering and tilting the specimen with the goniometer stage, which was carefully calibrated.

Calculation of the sputtering rate proceeds as follows. Let the projected width of a twin before sputtering be W_1, then the specimen thickness is $T_1 = W_1 \tan\alpha$. After irradiation the twin is now of true width $A'B$ where A' is a point inside the specimen, which represents the 'upper' edge of the twin. Thus $T_2 = W_2 \tan\alpha$, where T_2 is the thickness of the crystalline part of the specimen. The sputtering rate in a direction normal to the specimen plane is given by

$$R = \frac{T_1 - (T_2 + \Delta)}{t}$$

so

$$R = \frac{(W_1 - W_2)\tan\alpha - \Delta}{t} \qquad (2)$$

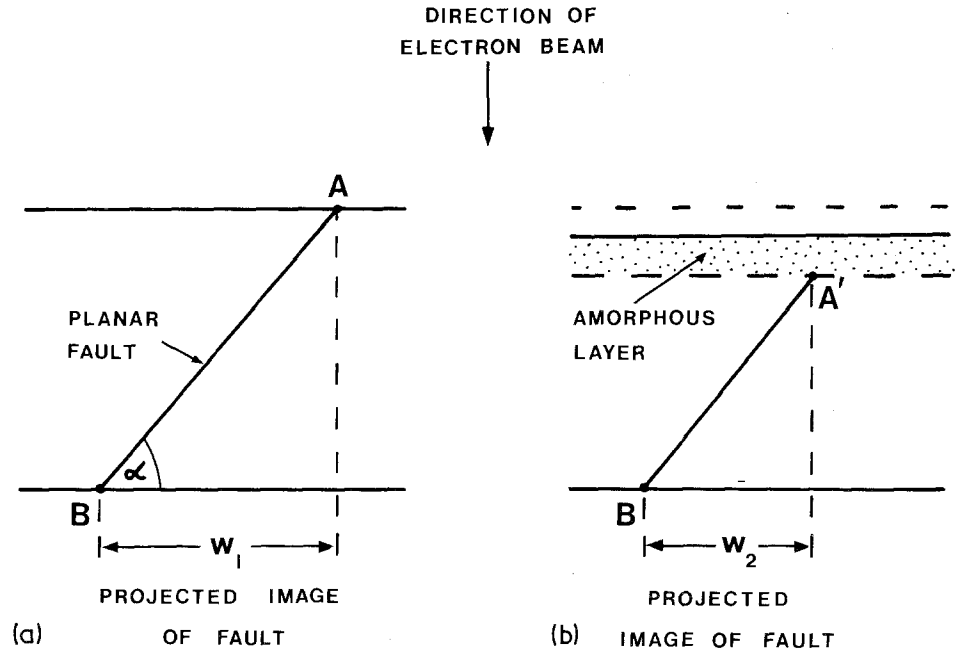

Figure 2 (a) Diagram to show section through a thin cleavage flake of carbonate containing a twin boundary, before ion irradiation. (b) Diagram to show the disposition of the same twin boundary and the surface layer of amorphous material after ion irradiation of the upper surface.

Δ must be determined by determining the depth of the point A' with respect to the reference point on the upper surface of the specimen after irradiation. The equations used for calculating Δ, utilizing polystyrene spheres to establish the reference points, are given in the Appendix.

Application of the method required that the magnification was known accurately and that the crystals could be set at known orientations in the electron microscope with considerable accuracy. The latter was achieved by using the array of Kikuchi lines which are produced by the multiple scattering of electrons and are seen in the diffraction pattern of a relatively thick crystal (see [26]). After sputtering the part of the crystal containing the twin to be remeasured was too thin to give Kikuchi lines but the orientation could nonetheless be set by making a small lateral translation to a thicker region. Kikuchi patterns were also used to effect calibration of the goniometer stage, mentioned above.

Convenient planar crystal defects exist in both calcite and dolomite in the form of twin boundaries and thin twin lamellae. In calcite the common twin plane is $\{0\,1\,\bar{1}\,8\}$ and in dolomite it is $\{0\,1\,\bar{1}\,2\}$*. The cleavage planes are $\{1\,0\,\bar{1}\,4\}$ in both carbonates and it is convenient that the cleavage of calcite commonly introduces numerous twins. The angles between the three possible $\{0\,1\,\bar{1}\,8\}$ twin planes in calcite and the $(1\,0\,\bar{1}\,4)$ cleavage plane are 52°, 52° and 14°. In dolomite the angles between the $\{0\,1\,\bar{1}\,2\}$ twin planes and the $(1\,0\,\bar{1}\,4)$ plane are 40°, $18\frac{1}{2}$°, $18\frac{1}{2}$°.

Flakes of the carbonates of suitable thickness for sputtering measurement were produced by cleavage and selected by optical microscopy. They were then mounted onto copper 'washer-type' grids with small amounts of epoxy cement. Prior to insertion into the electron microscope it was necessary to evaporate a thin (~ 20 nm) coating of carbon onto one side of the specimens to prevent charging in the electron beam. Specimens suitable for sputtering studies, i.e. having twins in regions of considerable thickness, were selected by preliminary examination in the electron microscope. The chosen twinned regions were photographed at a moderate magnification and selected area diffraction patterns taken at the 'cleavage' orientation, to be checked with standard trace analysis stereographic projections of twins for the appropriate

* Indices refer to the hexagonal structural unit cell with $c = 1.706$ nm and $a = 0.499$ nm for calcite; $c = 1.601$ nm and $a = 0.481$ nm for dolomite.

carbonate. Low magnification images were also recorded to ensure that the same region could be found again after sputtering, even though its appearance would be considerably altered. Further details of technique are given elsewhere [27]. The electron microscope used was a JEM 7, operated at 100 kV.

3. Results

3.1. Angular dependence of sputtering yield

The optical microscope method, (Section 2.2.2) was used to find how the sputtering yield varied with inclination of the ion beam to the crystal surface. Cleaved crystals were used and these were rotated in the plane of cleavage at 6 r.p.m. during ion bombardment in order (a) to obviate the need to set crystals in particular orientations, thus to eliminate possible channelling effects; (b) so that the results would best simulate the conditions used in ion-thinning when preparing samples for electron microscopy (see [28]).

The values of sputtering rate measured directly showed a sharp peak at a surface to ion beam inclination of 45°, but the maximum moves to approximately 70° when the results are multiplied by sec θ to apply the correct ion current density normal to the surface. (Clearly, both R and Δ are measured normal to the crystal surface.) The results are adjusted by the value of Δ, as measured by subsequent electron microscopy, although this amounts to a correction of only about 0.5% for sputtering times of $\sim 2 \times 10^2$ min (dose rate $\simeq 5 \times 10^{14}$ ions cm^{-2} sec^{-1}). Fig. 3 shows the angular dependence of yield for bombardment of the cleavage face of calcite.

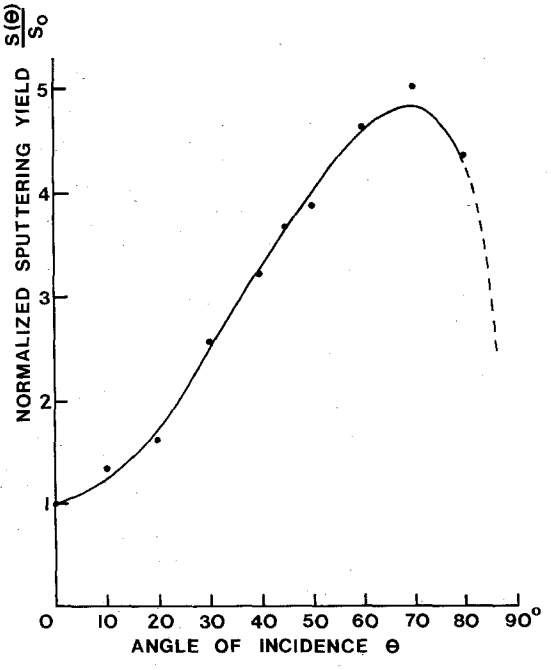

Figure 3 Angular dependence of sputtering yield for calcite crystal with $\{1\,0\,\bar{1}\,4\}$ cleavage faces irradiated at 5 kV.

The appearance of Fig. 3 is a function of the rotation of the crystals in their surface plane, as any strongly anisotropic effects such as channelling will have been averaged out. The result is probably very similar to that which would have been obtained if polycrystalline calcite could have been used. There is general similarity between the curve of Fig. 3 and results obtained on polycrystalline metals and by Bach [22] for silica-glass bombarded at 5.6 kV.

At this juncture, it should be emphasized that the values of sputtering yield given in Fig. 3 and elsewhere in this paper are only qualitative because the d.c. ion source used produces particles of more than one energy and species; also it is not pure because of cathode wear, etc. These points are discussed later (Section 4) but meanwhile the values on the right-hand ordinate should be recognized as obtained by taking a value of two for the factor γ (This is the estimated ratio of the number of neutrals to the number of ions in the beam [29]. Moreover, the particle energies for a source operated at 5 keV, peak at about 5 kV and there is also a broad peak at 1.5 keV because of inter-electrode collisions.

3.2. Dependence of sputtering ratio and thickness of amorphous layer on direction of ion beam

Since the rhombohedral carbonates are very anisotropic, it seems possible that the foregoing results, employing specimen rotation, mask strong directional effects. Furthermore, it could be envisaged that if strong channelling effects were present, these would not only affect the sputtering ratio, but might also affect the thickness of the amorphous layer, by changing the depth distribution of energy dissipation. These possibilities were investigated by the electron microscope method. Unfortunately, lack of time prevented a full exploration of all the crystal target directions which might have revealed channelling effects.

Before starting experiments, we considered the crystal structure of calcite to ascertain where

possible channels might lie. Inspection of the lattice shows that the directions $\langle 1\,1\,\bar{2}\,0\rangle$ and $\langle 4\,\bar{4}\,0\,1\rangle$ are likely channelling directions while, by contrast, irradiation perpendicular to the basal plane, (0 0 0 1), offers the ions a high packing density of target atoms. Other crystallographic directions may also lead to some channelling, but it was decided initially to seek for channels which might produce large variations in sputtering parameters.

The irradiations were carried out without rotation of the specimens, all of which were cleavage flakes of orientation $\{1\,0\,\bar{1}\,4\}$. The measurements of S and Δ were made by the electron microscope method and give values of these two quantities measured in a direction normal to $\{1\,0\,\bar{1}\,4\}$. The results given in Table I reveal startling variations in both S and Δ, with S a maximum and Δ a minimum for irradiation normal to the basal plane. The $\langle 1\,1\,\bar{2}\,0\rangle$ direction gave a value of Δ almost 2.5 times larger, while the sputtering yield was smaller by a factor of about seven. For this open channel direction it appears that most of the ions dissipate their energy over a considerable range, producing inefficient sputtering and consequently, a broad zone of damage. Specimen rotation, which is often used during the ion-thinning process to avoid the creation of cone structures, is clearly useful as a means of reducing the exposure along potential channelling directions. However, rotation is not feasible in all practical situations and we therefore decided to see what effect the temperature of the specimen had on sputtering characteristics and whether it might be used as an additional control.

3.3. Dependence on sputtering ratio and thickness of amorphous layer on target temperature

In the experiments to investigate the influence of specimen temperature we also sought to discover how long it took to establish an equilibrium sputtering condition. The need to study this aspect stemmed from the two following considerations. Firstly, it clearly takes time for a specimen to reach a stable temperature under a given flux of ions and during this time the sputtering yield may change if target temperature is an important variable in the loss of atoms from compound crystalline material during sputtering (of course, this is most likely to be an indirect sputtering effect). Secondly, there must be a certain minimum ion dose per unit volume of crystal to effect the transformation of a crystal to its amorphous state. Therefore, we can suppose that until an equilibrium thickness of amorphous material is established (the time for which will again depend on irradiation conditions and perhaps target temperature) the sputtering ratio may change with time. Thereafter the sputtering ratio is at least partly characteristic of the amorphous material, the nature of which we currently know little about.

The results obtained from this series of experiments are shown in Table II. Use of the electron microscope method to determine these values explains both their strengths and their weaknesses. Although Δ cannot be measured by other methods, each electron microscope result represents a considerable expenditure of effort (see Section 4). Therefore, it was not possible to make a number of measurements of Δ and S over small intervals of time, as would have been desirable to see how quickly a recognizable amorphous layer was created and how it varied in thickness with time in the early stages. The temperatures given in Table II are the recorded bulk temperatures of the specimens, which were cemented to relatively massive tables during irradiation. Unfortunately, they do not indicate the surface temperatures of the specimens, which would be of much greater significance in determining the sputtering parameters.

The results indicate, however, the existence of at least three important effects, which may be summarized as follows: the thickness of the amorphous layer at all three temperatures probably reached a maximum within 15 min of commencing bombardment and within a further 10 min attained a lower stable value. The values of the sputtering yields increased in an inverse manner with a similar time scale. The effect of lower temperatures was to decrease both the thickness of the amorphous layer and the values of sputtering yield. The latter effects are not to be expected in terms of current ideas on the mechanisms of sputtering and they suggest that complex processes involving chemical decomposition may be operative in irradiated carbonates.

4. Discussion

The foregoing results are interesting in that they illustrate both the potential strength of the electron microscope method used and point to some intriguing effects in the behaviour of ion-bombarded calcite. Undoubtedly the nature of the

TABLE I Measured values of the sputtering yield and thickness of the amorphous layer in specified crystallographic directions of calcite.

Direction $[UVTW]$	Angle ψ between $[UVTW]$ and direction normal to $(10\bar{1}4)$	Apparent amount R' sputtered in 25 min (10^{-2} μm)	Thickness of amorphous layer, Δ (10^{-2} μm)	Sputtering rate R, $[(R'-\Delta)\sec\psi]/25$ (10^{-2} μm min^{-1})	Number of atoms sputtered, N_s (10^{13} sec^{-1})	Sputtering yield (atoms per ion)	
						$S(1+\gamma)=N_s/N_i$	$S=N_s/3N_i$
[0001]	$44\frac{1}{2}°$	24.89	5.91	1.074	146.10	2.92	0.87
$[11\bar{2}0]$	52°	17.01	15.02	0.134	18.20	0.36	0.12
$[4\bar{4}01]$	52°	10.24	7.17	0.20	27.20	0.54	0.18

Ion energy = 5 kV, dose rate = 5×10^{14} ions cm^{-2} sec^{-1}.

TABLE II

Temperature (K)	Irradiation time (min)	Apparent amount R' sputtered in t min (10^{-2} μm)	Thickness of amorphous layer, Δ (10^{-2} μm)	Sputtering rate $R=(R'-\Delta)/t$ (10^{-2} μm min^{-1})	Number of sputtered atoms, N_s ($N_s \times 10^{13}$ sec^{-1})	Sputtering yield	
						$S(1+\gamma)=N_s/N_i$ (atoms per ion)	$S=N_s/3N_i$ (atoms per particle)
293	15	7.90	2.40	0.37	50.3	1.01	0.34
	25	13.00	1.00	0.48	65.3	1.31	0.43
	25*	13.40*	0.90*	0.50*	78.0*	1.56*	0.52*
	60	33.00	1.00	0.53	72.5	1.45	0.48
203	15	5.90	1.70	0.28	38.1	0.76	0.25
	25	9.80	0.60	0.37	51.8	1.01	0.34
	60	25.20	0.60	0.41	55.8	1.12	0.37
77	15	3.40	0.40	0.20	27.2	0.54	0.18
	25	5.70	0.07	0.23	30.9	0.62	0.21
	60	13.20	0.07	0.22	29.8	0.60	0.20

*Results for single crystals of dolomite.

amorphous layer is intimately connected with some of the observed effects. While its existence and the order of its thickness is now clearly established, a better understanding of its chemical composition and structual characteristics would be a great asset in interpreting the results.

Starting with the angular dependence of sputtering yield, our results hold no surprises, for the shape of the curve obtained is generally similar to that obtained for other materials which approximate to random solids. Indeed, with the knowledge of the amorphous surface layer extending to depths as great as 15 nm, which is considerably greater than the typical length of the cascade processes normally thought to be induced by low energy ions, we might view calcite as becoming truly random within a few minutes of commencing bombardment. The results of the channelling experiments, however, must be interpreted as showing that this picture is too simple. For if there was a truly random surface layer extending to the maximum range of the incident ions, no channelling effects would be detected. A way out of the apparently contradictory results seems to require a layer of damaged material which is sufficiently disordered to give only very weak diffraction contrast effects in the electron microscope (there are very faint bend contours visible in the central region of Fig. 1a), but yet retains sufficient relicts of the earlier calcite structure to promote channelling to considerable depths.

It is interesting to note that in carbonates the lattice damage caused by ions and by electrons differs markedly in appearance, while in many metals and in certain inorganic compounds both electrons and heavy particles produce damage in the form of defect clusters and dislocation loops. In fact, in reactor materials electron radiation damage studies have been used to simulate the effect of heavier radiations. Electron damage in carbonates, and in calcite in particular, manifests itself as spotty contrast in the electron microscope, with the rapid growth of loops. Prolonged electron irradiation in the microscope, probably aided by the consequent rise in specimen temperature, leads to the decompostion of calcite to calcium oxide, CaO, with loss of CO_2. In contrast, ion-irradiated samples have never been found to exhibit any trace of defect clusters or loop damage when first viewed in the electron microscope. This must indicate that the amorphous layer, which *a fortiori,* cannot reveal its structure by any scattering mechanism which utilizes elastically-scattered electrons, embraces the total extent of radiation damage in the carbonates. Of course, the layer's very considerable thickness also makes this likely. We have no direct evidence of the loss of carbon dioxide from the amorphous layer under the irradiation conditions which we normally employ and which are recorded above. However, prolonged irradiation at higher dose rates ($\sim 5 \times 10^{17}$ cm^{-2} total) has been found to produce diffraction spots characteristic of calcium oxide, suggesting that some loss of CO_2 must also occur at lower dose rates.

The change in the thickness of the amorphous layer with time, reported in Section 3.3, is perhaps what one might anticipate from the most simple arguments. The apparent decrease of Δ with time and the increase of S with time could be explained by assuming that as the subsurface zone becomes increasingly random, most of the incident ions are less able to effect a deep penetration without significant energy loss. As the average depth of the sites of principle momentum transfer processes is reduced, there is a greater probability of escape of the struck particles and S increases. The greater yield rate thus in turn contributes to a reduction of Δ. A further enhancement of the sputtering yield is introduced, as the equilibrium level of radiation damage becomes established, though the reduction in chemical co-ordination and consequent reduction in the binding energy.

The aspect of our results which is more difficult to explain in detail is the variation of both Δ and S with target temperature. Our belief is that the only consistent view is that here our observations relate, strictly speaking, to thermal decomposition of carbonate and not to the primary sputtering process. We can envisage the removal of matter by sputtering as a two part process in carbonates – the customary back scattering of subsurface target atoms, accompanied by the loss of volatile CO_2 by diffusion through the disrupted structure. This would imply that the amorphous zone is rich in CaO but it would only be able to appear as an identifiable second phase if the ambient temperature were sufficiently high to permit recrystallization. We are effectively proposing that diffusion of the species CO_2 is significant, but that Ca atoms are not mobile, except in transient cascades. Viewed from the standpoint of this model, the thickness of the amorphous zone is not merely a measure of the depth of penetration of incident

ions, but is a measure of the diffusion length for CO_2 in a radiation-damaged carbonate structure at various temperatures. As a consequence of this interpretation, we could anticipate that the detailed structure of the amorphous layer will vary with temperature and with the flux of bombarding ions. In any irradiated crystalline material this will have some truth because of implantation effects, but is should be especially true in compounds with decompose. The decomposition of such compounds and therefore their overall sputtering behaviour will be temperature sensitive under carefully chosen irradiation conditions.

The results which we report are not as extensive as we would have liked. But it must be stressed that obtaining results by the electron microscope method is time-consuming because of the fairly high chance of failing to be able to make a second thickness measurement after irradiation. This can arise from specimens failing by fracture, sputtering away of the reference area or failing to recognize it, or chance mishandling of the fragile samples. We further feel that while the results usefully point to certain effects worthy of more investigation, there is dubious value in making more measurements until the results can be made quantitative by use of a more sophisticated ion source.

As mentioned earlier in Section 3.1, the d.c. ion source used by us is not monoenergetic and produces ions in two main energy peaks. One peak corresponds to ions of energy corresponding to the applied voltage. The other peak corresponds to ions which have made collisions within the low vacuum inter-electrode space in the ion source. These collisions also produce charge exchanges so that a high percentage of neutral particles also move with the ion beam, carrying energies corresponding to the position of the lower energy peak. The characteristics of this type of ion source have been considered by Crockett [29], and his work has been used in estimating the ratio of neutral particles to singly charged ions in our own ion beam. The ratio, γ, has been generously estimated as equal to two and the uncertainty in this figure is unfortunately reflected in the calculated values for S. Other sources of error are as follows: the values of R and Δ measured by electron microscopy are estimated as accurate to $\pm$ 5%. The measurements of R with the polarizing microscope have an error of $\pm$ 4%. The measurements of dose are accurate to $\pm$ 3%.

Despite the above limitations to our work, the values of S calculated for room temperature irradiation are in fair agreement with the measurements of Bach [22] for $CaCO_3$ bombarded with 5.6 keV argon ions. The values we obtain, like those of Bach, are very much lower (by about an order of magnitude) than values obtained by our own calculations [27], using the theory of Sigmund [31].

Acknowledgements

One of us (JA) would like to thank the Nigerian Government for a grant during the period of this work. We would both like to thank P. Vincenzi for technical assistance, G. Carter and I.S.T. Tsong for helpful criticisms of this paper.

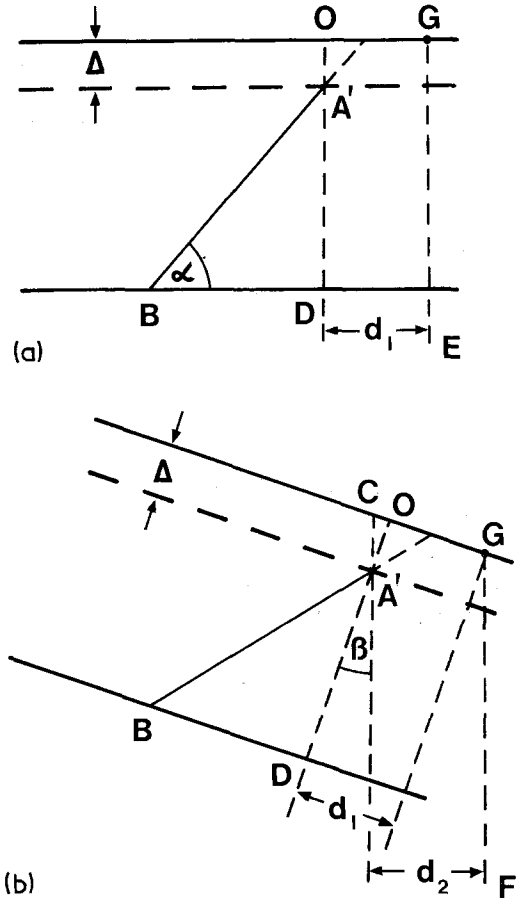

Figure 4 (a) Illustrating the disposition of a crystal specimen, and internal planar fault (twin boundary) for Case 1, before tilting the goniometer stage. (b) Illustrating the disposition of the crystal and planar fault for Case 1 after tilting the goniometer stage through an angle of + β about an axis parallel to the line of intersection of the fault and with the specimen surface.

Appendix

The method of determining the amorphous layer thickness, Δ, is derived from the stereomicroscopy method of Diepers and Diehl [32]. Two micrographs of the specimen are taken; one with a tilt angle of $+\beta$, the other with a tilt angle of $-\beta$, both measured from a reference orientation in which the specimen surface is normal to the electron beam. The tilt axis must be parallel to the intersection of the twin plane with the specimen surface.

The position of A' is then determined from the change in the projected distance between the reference point G and the point A' on the edge of the twin. Two possible positions G and G' of the reference point must be considered:

Case 1; reference point adjacent to A'. The electron beam is normal to the plane of the specimen in Fig. 4a, while a tilt of $+\beta$ has been applied in Fig. 4b. Points E and F represent the projected positions of the reference point G for tilt angles of 0 and $+\beta$ respectively.

Then

$$\tan\beta = \frac{CO}{OA'}$$

but

$$CO = d_2 \sec\beta - d_1 \quad \text{and} \quad OA' = \Delta$$

where d_1, d_2 are the projected lengths of $A'G$ at the two angular settings.

$$\therefore \Delta = (d_2 \sec\beta - d_1)\cot\beta$$

$$\text{i.e. } \Delta = \frac{d_2 - d_1\cos\beta}{\sin\beta} \qquad (3)$$

If a tilt of $-\beta$ is applied, the projected length of $A'G$ is less than at zero tilt. Taking the absolute value of β, the corresponding equation to Equation 3 becomes

$$\Delta = \frac{d_1\cos\beta - d_3}{\sin\beta} \qquad (4)$$

Case 2; reference point adjacent to B. Derivations comparable to Case 1 are possible, giving the equations:

$$OD = \frac{d_2' - d_1'\cos\beta}{\sin\beta} \text{ for } +\beta \text{ tilt} \qquad (5)$$

$$OD = \frac{d_1'\cos\beta - d_2'}{\sin\beta} \text{ for } -\beta \text{ tilt}$$

The thickness of crystalline specimen is

$$T_2 = W_2\tan\alpha$$

$$\therefore \Delta\frac{d_2' - d_1'\cos\beta}{\sin\beta} - W_2\tan\alpha, \text{ for } +\beta \text{ tilt}$$

$$\text{and } \Delta = \frac{d_1'\cos\beta - d_2'}{\sin\beta} - W_2\tan\alpha, \text{ for } -\beta \text{ tilt.}$$

References

1. G. CARTER and J. S. COLLIGON, "Ion Bombardment of Solids" (Heinemann Educational Books Ltd., London, 1968) p. 37.
2. P. SIGMUND, *Rev. Roumaine Phys.* **17** (1972) 1079.
3. *Idem*, "Physics of Ionized Gases", edited by M.V. Kurepa (Institute of Physics, Boegrad, 1972) p. 137.
4. H. OECHSNER, *Appl. Phys.* 8 (1975) 195.
5. I. S. T. TSONG and D. J. BARBER, *J. Mater. Sci.* 8 (1972) 123.
6. Yu. V. MARTYNENKO, Proceedings of the Conference on Atomic Collision Phenomena in Solids, edited by D. W. Palmer, M. W. Thompson and P. D. Townsend (North Holland, Amsterdam, 1970) p. 400.
7. D. S. GEMMELL, *Rev. Mod. Phys.* **46** (1974) 129.
8. G. CARTER and W. A. GRANT, "Ion Implantation in Semiconductors" (Edward Arnold, London 1976) p. 68.
9. U. GIANOLA, *J. Appl. Phys.* **28** (1957) 868.
10. D. J. MAZEY, R. S. NELSON and R. S. BARNES, *Phil. Mag.* **17** (1968) 1145.
11. R. J. MACDONALD, *ibid* **21** (1970) 519.
12. I. H. WILSON, *Rad. Effects.* **18** (1973) 95.
13. N. HERMANNE and A. ART, *ibid* **5** (1970) 203.
14. D. J. BARBER and H. R. WENK, "Electron Microscopy in Mineralogy", edited by H. R. Wenk, (Springer–Verlag, 1976) p. 428.
15. J. BORG, J. C. DRAN, L. DURRIEU, C. JOURET and M. MAURETTE, *Earth Planet Sci. Lett.* 8 (1970) 379.
16. P. STAIB, *Rad. Effects* **18** (1973) 217.
17. PUTNIS, Private communication, 1977.
18. H. M. NAGUIB and R. KELLY, *Rad. Effects* **25** (1975) 1.
19. M. L. TARNG and G. K. WEHNER, *J. Appl. Phys.* **42** (1971) 2449.
20. J. M. POATE, W. L. BROWN, R. HOMER, W. M. AUGUSTYNIAK, J. W. MAYER, K. N. TU and W. F. VAN DER WEG, *Nucl. Instr. Methods* **132** (1976) 345.
21. P. S. HO, J. E. LEWIS, H. W. WILDMAN and J. K. HOWARD, *Surface Sci.* **57** (1976) 393.
22. H. BACH, Nucl. Instr. Methods **84** (1970) 4.
23. W. BRANDT and A. R. LAUBERT, *ibid* **47** (1967) 201.
24. P. LERVIG, J. LINDHARD and V. NIELSON, *Nucl. Phys. A.* **96** (1967) 481.
25. N. H. HARTSHORNE and A. STUART, "Crystals and the Polarizing Microscope", 4th edition (Edward Arnold, London, 1970) p. 126.

26. P. B. HIRSCH, A. HOWIE, R. B. NICHOLSON, D. W. PASHLEY and M. J. WHELAN, "Electron Microscopy of Thin Crystals", (Butterworths, London, 1965) p. 119.
27. J. ADETUNJI, PhD Thesis, University of Essex, 1976.
28. D. J. BARBER, *J. Mater. Sci.* **5** (1970) 1.
29. C. G. CROCKETT, *Vacuum* **23** (1972) 11.
30. B. J. BURRAGE and D. R. PITKETHLY, *Phys. Stat. Solidi.* **32** (1969) 399.
31. P. SIGMUND, *Phys. Rev.* **184** (1969) 383.
32. H. DIEPERS and J. H. DIEHL, *Phys. Stat. Solidi.* **16** (1966) 109.

Received 22 June and accepted 22 July 1977.